Published in final edited form as:
Nat Med. 2018 September ; 24(9): 1324–1329. doi:10.1038/s41591-018-0103-x.

Biochemical autoregulatory gene therapy for focal epilepsy

Andreas Lieb[*], **Yichen Qiu**, **Christine L Dixon**, **Janosch P Heller**, **Matthew C Walker**, **Stephanie Schorge**, and **Dimitri M Kullmann**[*]
Department for Clinical and Experimental Epilepsy, UCL Institute of Neurology, University College London

Abstract

Despite the introduction of over a dozen new antiepileptic drugs in the last 20 years, approximately one third of people who develop epilepsy continue to have seizures on mono- or polytherapy1. Viral-vector mediated gene transfer offers the opportunity to design a rational treatment that builds on mechanistic understanding of seizure generation and that can be targeted to specific neuronal populations in epileptogenic foci2. Several such strategies show encouraging results in different animal models, although clinical translation is limited by possible effects on circuits underlying cognitive, mnemonic, sensory or motor function. Here we describe an autoregulatory anti-epileptic gene therapy, which relies on neuronal inhibition in response to elevations of extracellular glutamate. It is effective in a rodent model of focal epilepsy, and well tolerated, thus lowering the barrier to clinical translation.

Around 70 million people worldwide are affected by epilepsy, of whom approximately 30% continue to have seizures despite optimal medical treatment3,4. Antiepileptic drugs have a narrow therapeutic window, mainly because they do not differentiate between neurons involved in seizure generation and those underlying normal brain function5. The most effective treatment option for refractory focal-onset epilepsy is surgical resection, but this is restricted to cases where the epileptogenic zone is relatively far from eloquent cortex6. Gene therapy to reduce neuronal excitability has shown promise in preclinical models, but is also irreversible, limiting clinical translation. On-demand gene therapy with optogenetics7 or chemogenetics8 can address this issue but faces additional translational obstacles because of the need for continuous EEG monitoring and devices for light or ligand delivery. Efficient algorithms for seizure forecasting are available but are associated with an appreciable rate of

[*]Corresponding Authors: a.lieb@ucl.ac.uk, d.kullmann@ucl.ac.uk.

Author Contributions:
AL and DMK designed all experiments and drafted the manuscript. AL performed *in vitro* electrophysiology and *in vivo* experiments. AL and YQ designed, performed, and analysed *in vivo* behavioural experiments. YQ, AL, JPH, and CLD performed and analysed all immunostaining experiments. AL, YQ, JPH, CLD, MCW, SS and DMK revised the manuscript.

Competing financial interests
The authors declare no competing financial interests.

Life Sciences Reporting Summary.
Further information on experimental design is available in the Life Sciences Reporting Summary.

Data and code availability statement.
Data and code are available upon request.

Europe PMC Funders Author Manuscripts

false positives9,10. Furthermore, both EEG monitoring and light or ligand delivery require implanted devices, which are associated with surgical risks, post-operative complications, finite lifetime, and interference with MRI. Chemogenetics can potentially be used on a slower timescale, with exogenous ligand delivery by an oral or parenteral route, but this too may interfere with normal brain function for the duration of the therapeutic effect. We therefore aimed to develop a molecular tool to inhibit neurons in response to pathological accumulation of extracellular glutamate, a hallmark of excessive synchronous discharges of excitatory neurons in seizures (Fig. 1a)11–15.

For this purpose we designed a viral plasmid coding for a fully codon-optimized glutamate-gated Cl^--channel (GluCl from *C. elegans*), where the α-subunit is linked via a self-cleaving viral 2A-peptide to the GluCl β-subunit, with mYFP in the M3-M4 loops of both subunits16. The leucine residue at position 9 of the M2 pore-forming domain of the wild type GluCl α-subunit was mutated to phenylalanine in order to enhance the channel's glutamate sensitivity16 (enhanced GluCl or eGluCl). To bias expression of eGluCl to excitatory neurons, eGluCl was placed under the control of the human CaMKIIα promoter (hCamKII)17 (Fig. 1a). Subsequent full electrophysiological characterization in Neuro-2a cells confirmed that the EC_{50} for glutamate was decreased from 262±53μM (wild type GluCl, n=8, mean±sem) to 12±3μM (eGluCl, n=8) ($p<0.001$, Student's t-test) (Fig. 1b), comparable to extracellular glutamate levels detected during seizures13,15.

Following eGluCl lentivector packaging (titer $2.15*10^9$TU/ml) we assessed its transduction efficiency *in vivo*. We therefore injected adult male Sprague Dawley rats with either eGluCl or GFP control lentivector into the primary motor cortex (M1), and looked for expression after 7 days. eGluCl was mainly detected at extrasynaptic locations (Supplementary Fig. 1), as estimated by very limited co-localization with the synaptic marker PSD95: 0.29±0.01% of eGluCl occurred at PSD95 puncta, and conversely 13.50±2.49% of PSD95 co-localized with eGluCl in transduced areas of the brain (Pearson's correlation coefficient: 0.19±0.03, n=3 independent animal brain preparations) (Fig. 1c). Given that glutamate is efficiently cleared from the extrasynaptic space by excitatory amino acid transporters14,18,19, these results suggest that eGluCl should have a minimal impact on normal brain-function. eGluCl was expressed at the earliest time point evaluated (day 3 post-injection), and persisted for at least 245 days, consistent with other lentivectors20 (Fig. 1d).

We assessed the ability of eGluCl to attenuate seizures evoked by acute intracortical administration of the chemoconvulsant pilocarpine8. For this purpose, we implanted adult male Sprague Dawley rats with a wireless transmitter, with an electrode in M1, and secured a cannula for access to same brain region. One week after surgery, we injected pilocarpine via the cannula and quantified the evoked seizure severity. Subsequently, the animals were treated with an equivalent dose of either eGluCl or a control lentivector expressing green fluorescent protein, hCaMKII-GFP (GFP). The chemoconvulsant injection was then repeated in a randomized and blinded study, comparing the effect of pilocarpine before (pre-Rx) and 14 days after lentiviral treatment (post-Rx) with either lentivector into the same region of the rat motor cortex (Fig. 2A). Animals treated with eGluCl exhibited a decrease in the electrocorticogram (ECoG) coastline, an aggregate of frequency and amplitude, between the two pilocarpine injections (absolute change in coastline: –1.08±0.58V at 20 minutes,

n=6). In contrast, GFP-treated animals exhibited an increase in coastline between the two pilocarpine injections (1.04±0.34V, n=7; comparison between eGluCl and GFP: p=0.007, Student's t-test; Fig. 2b). Comparison of the number of large amplitude ECoG spikes (>25% of the maximum amplitude evoked by pilocarpine) also revealed a pronounced effect of eGluCl (ratio of spikes in the second trial to the first trial: eGluCl 0.60±0.12; GFP 1.27±0.18; p=0.012). Similarly, ECoG power in the 4–14Hz frequency band, which correlates with motor convulsion severity8 (Supplementary Video 1), decreased in eGluCl treated animals (ratio of second trial to first: 0.44±0.19), but increased in GFP-treated animals (1.47±0.16; p=0.002). Finally, the spike frequency decreased after eGluCl treatment (ratio: 0.65±0.13) in contrast to GFP-treated animals (ratio: 1.29±0.14; p=0.007). The total duration of pilocarpine-evoked electrographic seizure activity, which is mainly determined by the clearance of the chemoconvulsant from the brain, showed a non-significant trend towards a decrease in eGluCl-treated animals (ratio: 0.79±0.11) compared to GFP-treated animals (1.02±0.10; p=0.146) (Fig. 2c, Supplementary Fig. 2). eGluCl is thus effective at attenuating acute chemoconvulsant-evoked seizures.

We next determined the effect of eGluCl in a model of chronic focal neocortical epilepsy induced by tetanus toxin injection into the visual cortex21. In this model spontaneous seizures occur over several weeks (Fig. 3a, b, Supplementary Video 2, Supplementary Fig. 3a). eGluCl or GFP lentivectors were injected 11 days after tetanus toxin injection in a randomized and blinded study design. The number of seizures prior to treatment did not differ between the groups (eGluCl 10.1±1.5, n=10; GFP 10.4±1.2, n=10; p=0.761, Student's t-test) (Fig. 3d inset). eGluCl significantly reduced the number of subsequent seizures in comparison to GFP-treated animals (generalized log-linear mixed model: $F(1, 59)=20.66$, treatment effect $p<0.001$; $F(8, 59)=17.28$, treatment*week interaction effect $p<0.001$) (Fig. 3c). The cumulative number of seizures normalized by the number of pre-Rx seizures was also significantly reduced (eGluCl: 2.62±0.26, n=10; GFP: 3.79±0.24, n=10; p=0.004, Student's t-test) (Fig. 3d), as was the absolute number of seizures experienced per animal post-Rx (eGluCl: 16.2±2.9, n=10; GFP: 28.9±4.4, n=10; p=0.034, Mann Whitney test) (Supplementary Fig. 3b). We did not, however, observe a significant difference in average seizure duration (eGluCl 85.6±53 sec, n=9; GFP 94.3±4.7 sec, n=10; p=0.278, Mann Whitney test; note that one eGluCl-treated animal did not experience any seizures post-Rx) or severity (Supplementary Fig. 3b, c), consistent with evidence that seizure duration is mainly determined by the extent of the network involved rather than by activity at the focus22.

We asked if eGluCl treatment affects interictal activity by comparing the absolute ECoG coastline after discarding all seizures. This revealed a steep increase following tetanus toxin injection, and no difference between eGluCl- and GFP-treated animals (Fig. 4a). eGluCl is thus effective in reducing spontaneous seizure frequency without altering the baseline ECoG.

To look for off-target effects of eGluCl on normal brain function, we injected another group of non-epileptic animals with either lentivector and asked if the ECoG was affected. The average of 6h ECoG coastline (0:00 – 6:00AM) 2 weeks post-Rx, expressed as a ratio of pre-Rx ECoG, did not differ between treatment groups (ratio: eGluCl: 1.01±0.03, n=7; GFP:

1.06±0.03, n=6; p=0.293, Student's t-test). As a positive control, in a further group of animals, we administered ivermectin (IVM, 5mg/kg IP), an activator of GluCl23. This significantly reduced the coastline in animals treated with eGluCl compared with GFP (ratio: eGluCl: 0.93±0.04, n=6; GFP: 1.10± 0.03, n=5; p=0.010, Student's t-test) (Fig. 4b).

In order to look for behavioral effects of eGluCl, we assessed performance in two tests of motor coordination sensitive to motor cortex lesions, again blind to treatment, after injection of eGluCl or GFP lentivector into layer 5 of the motor cortex. No significant difference was seen in the accelerating rotarod test between groups (average latency to fall in 3 rotarod sessions eGluCl: 84.8±12.0sec, n= 5; GFP: 75.4±15.0 sec, n=6; p=0.646, Student's t-test). We also observed no significant difference in the average number of steps taken while the same animals walked on an elevated grid during 3 sessions (eGluCl: 83.5±12.7; GFP: 95.3±17.5; p=0.612, Student's t-test). Finally, we repeated the evaluation of motor coordination in the same animals after IVM. This revealed a robust difference between eGluCl and GFP when the latency to fall post-IVM was expressed as a ratio of the earlier test sessions pre-IVM (eGluCl: 1.36±0.12, n = 5, GFP: 0.96±0.05, n=6; p=0.009, Student's t-test; Fig. 4c). Although unexpected, a similar paradoxical increase in latency to fall has previously been reported with M1 lesions24. IVM also led to a marked decrease in the number of steps taken on the elevated grid by eGluCl-treated animals but not by GFP-treated animals (expressed as a ratio of steps taken pre-IVM, eGluCl: 0.76±0.09, n = 5; GFP: 1.04±0.08, n=6; p=0.045; Fig. 4d). In a separate cohort of animals that did not receive IVM we observed no significant difference on either test up to 25 days post-Rx (rotarod: two-way ANOVA, $F(1,56)=0.72$; steps: two-way ANOVA, $F(1,56)=0.37$; eGluCl, n=5; GFP, n=4) (Supplementary Fig. 4). We therefore conclude that eGluCl has no major impact on normal brain function, although an effect can be revealed by direct activation of the receptor by IVM, implying that the tests of motor coordination were sensitive to an increase in chloride conductance in transduced neurons.

Taken together, these results demonstrate that gene therapy with eGluCl is well tolerated and effective. Extrasynaptic glutamate is normally clamped to sub-micromolar concentrations by active transport19. Glutamate transporters nevertheless have a finite capacity to prevent extrasynaptic escape of the neurotransmitter25. eGluCl channels therefore only open in response to elevated extrasynaptic glutamate as occurs during seizures26. Chloride-permeable channels inhibit both by hyperpolarizing neurons and by decreasing the effective membrane resistance (voltage and shunting inhibition respectively). A collapse of trans-membrane chloride gradients has been reported in seizure models27, compromising voltage inhibition, but the robust anti-epileptic effect of eGluCl implies that shunting inhibition persists. This mechanism of action is shared with benzodiazepines and barbiturates, although these drugs potentiate the action of $GABA_A$ receptors indiscriminately, contributing to their narrow therapeutic window. Gene therapy with eGluCl thus represents a form of biochemical closed-loop chemogenetic treatment that does not require an exogenous agonist, and is therefore a promising approach to treat refractory epilepsy where the seizure focus is close to eloquent cortex.

Methods

Molecular biology

Lentiviral transfer plasmids were constructed using standard molecular cloning techniques. Wild type GluCl (GluCl α-subunit accession number: G5EBR3, β-subunit: Q17328) including the endoplasmic reticulum retention motif mutation RSR->AAA16 was fully codon optimized for human expression and synthesized by Genscript®. The L9'F mutation was inserted with the Quick Change II kit (Agilent). All plasmids were verified by sequencing before use (Source Bioscience). Sequences are available upon request. Lentivector were produced by Cyagen Biosciences Inc.

Voltage clamp recordings

In order to record GluCl Cl^- conductance, under the control of a human CamKII-α promoter, we used a mouse Neuroblastoma cell line (Neuro-2a). Heterologous expression of GluCl or eGluCl was obtained with TurboFect™ transfection reagent (Thermo Fisher Scientific). Whole cell patch clamp recordings were performed using Borosilicate glass electrodes, pulled on a micropipete puller (Sutter Instruments) and fire polished (Narishige), with a final resistance of 2-3.5MΩ. Data were digitized at 5kHz, filtered at 1kHz and recorded with WinEDR software (John Dempster, Glasgow, UK) and an Axopatch 1-D amplifier (Axon Instruments). Series resistance compensation of 60% was used throughout. Cells were held at -60mV, and increasing concentrations of glutamate were applied through a custom-built single-cell perfusion system. All recordings were performed at room temperature. The extracellular recording solution contained in mM: 150 NaCl, 2.8 KCl, 2 Ca_2Cl, and 10 HEPES, pH adjusted to 7.35 with NaOH, with glutamate as indicated, and the intracellular recording solution contained: 135 CsCl, 10 Cs-EGTA, 10 HEPES, 1 Mg_2Cl, and 4 Na_2-ATP, pH adjusted to 7.35 with CsOH.

Surgical procedures

All experiments were performed in accordance with the United Kingdom Animal (Scientific Procedures) Act 1986 approved by the Home Office (License PPL70-7684). All animals were kept under a 12h dark/light cycle (dark: 7PM – 7AM) at a constant temperature of 21°C and a humidity of 50%. Male Sprague-Dawley rats (275–350g) were anesthetized with isoflurane and placed in a stereotactic frame (Kopf). A cannula (Plastics One) and an ECoG electrode (Open Source Instruments) were placed in either the forelimb area of the right primary motor cortex (coordinates, 2.4 mm lateral, 1.0 mm anterior of bregma), or the right visual cortex (coordinates, 3.0 mm lateral, and 7 mm posterior of bregma). An ECoG transmitter (A3028E; Open Source Instruments) was implanted subcutaneously, to allow wireless telemetry recordings. The reference electrode was implanted in the contralateral hemisphere. For the chronic visual cortex tetanus toxin model, 15ng of tetanus toxin was injected in a volume of 1.0μl PBS at a rate of 200nl min^{-1} in layer 5 region. The Hamilton syringe (needle gauge 33) was held in place for 10 min after the injection.

Chemoconvulsant seizure model

After a week of recovery period from surgery, animals were injected on four consecutive days with increasing amounts (200, 450, 700, and 950nl) of 3.5mM pilocarpine solution in PBS into layer 5 of the right primary motor cortex at a rate of 100nl min^{-1} (the Hamilton syringe was held in place for 2 min post-injection). Three days later all animals were injected with 2.0μl of lentivector at the same location and a rate of 200nl sec^{-1} (1.0μl at -1.1mm and 1.0μl at -1.0mm from pia; the Hamilton syringe was held in place for 5 min and 10 min after virus injection, respectively). After waiting two weeks for transgene expression, the chemoconvulsant injection procedure was repeated. This experimental design allowed us to normalize every pilocarpine-evoked seizure to its corresponding pre-treatment seizure. In order to minimize inter-animal susceptibilities to different doses of pilocarpine, we averaged the normalized values across the different doses, rejecting any dose that was below threshold for seizure induction. Virus injection and subsequent data analysis was performed by a researcher blinded to treatment.

Chronic tetanus toxin epilepsy model

Eleven days after ECoG transmitter and tetanus toxin injection, animals were injected with 2.0μl of lentivector at a speed of 200nl sec^{-1} (1.0μl at -1.1mm and 1.0μl at -1.0mm from pia, the Hamilton syringe was held in place for 5 min and 10 min respectively after virus injection) into layer 5 of the right visual cortex. Virus injection and subsequent data analysis were performed by a researcher blinded to treatment.

ECoG acquisition and analysis

The ECoG was acquired wirelessly using hardware and software from Open Source Instruments, Inc. The ECoG was sampled at a frequency of 512Hz, band-pass filtered between 1 and 160Hz, and recorded continuously for the duration of the experiments.

ECoG analysis in the pilocarpine induced acute model of seizures was performed as previously described 8. Briefly, the coastline, the number of spikes reaching at least 25% of the maximal amplitude recorded within the seizure, 4–14Hz power, seizure duration, and inter-spike interval were calculated from raw traces imported into Python 3.5 (Supplementary Video 1). Values obtained for each dose of pilocarpine after lentivector treatment were compared to the corresponding values obtained for the same dose of pilocarpine prior to lentivector injection within each animal. The coastline analysis is shown as absolute difference, but other measures are shown as ratios for clarity.

The analysis of the chronic tetanus toxin induced model was performed as previously described7,8. Briefly, the ECoG was segmented into consecutive 1sec epochs and 6 different metrics calculated (coastline, power, intermittency, coherence, asymmetry, and the power between 20 and 50Hz) (Supplementary Video 2). Each metric was mapped onto the interval 0–1, yielding a point in a 6-dimensional hypercube of unit side. Each epoch was compared to a user-generated seizure library, consisting of seizures validated from at least 3 different animals. If the Euclidean distance between the coordinates for the epoch fell within 0.2 of a validated seizure-epoch, it was classed as a possible seizure. After successful detection of at least 3 seizures per animal, animal-specific seizure libraries were generated. Each seizure

Europe PMC Funders Author Manuscripts

which was not qualified by at least 6 potential seizure-events was added to the animal-specific seizure library. For Fig. 3, the number of seizures in each animal was normalized by the number of seizures during 1 week pre-treatment, to compensate for inter-animal variability. Raw, non-normalized, data are shown in Supplementary Fig. S3. For all datasets the minimal duration to define a seizure was set to 10sec.

Behavioral analysis

Rats injected with either eGluCl or GFP lentivector into the right motor cortex (long term study), or both hemispheres (study involving ivermectin as positive control) (M1 region layer 5, volume and coordinates as above) were assessed with the rotarod and elevated grid tests of motor coordination.

For the rotarod test (Ugo Basile), the rotation velocity increased from 3 to 30rpm over 5 minutes. The animals were habituated for 2 training sessions on the rotarod, each of which consisted of three trials. In the test sessions the latency to fall was recorded for three consecutive trials, and the best performance used for statistical analysis. For the elevated grid test, rats were placed on a 52x32cm elevated horizontal platform consisting of a square painted steel wire array (4mm diameter, 4cm spacing) and allowed to explore the arena for 2 minutes. All animals were allowed to habituate to the test environment for two consecutive days before the test sessions. Rats were video-monitored from two different angles, and the number of steps was counted.

One group of animals was assessed on three consecutive days on both tests prior to lentivector injection, and then on 8 subsequent sessions over the next 4 weeks. Another group of animals was treated with eGluCl or GFP lentivector 7 days prior to two habituation sessions on consecutive days, followed by three test sessions, and three further sessions after ivermectin injection (5 mg/kg, each given 24h prior to testing). All experiments and subsequent data analysis were performed by a researcher blinded to the treatment.

Immunohistochemistry

Staining was performed on free-floating 30 or 50μm rat brain sections with the following antibodies: mouse Anti-PSD95 (ab2723, Abcam), rabbit anti-GFP (ab6556, Abcam), guinea pig anti-MAP2 (Cat 188 004, Synaptic Systems), anti-Neurofilament heavy polypeptide (ab8135, Abcam), Alexa Fluor® 488 donkey anti-rabbit (A-21206, ThermoFisher Scientific), Alexa Fluor® 405 goat anti-guinea pig (ab175678, Abcam) and CF™568 Donkey anti-mouse (20105, Biotium). Images were acquired using ZEN software (Zeiss) on a LSM710 confocal microscope (Zeiss). Colocalisation of PSD95 and eGluCl analysis was performed via ImageJ1.51n (Wayne Rasband, National Instititue of Health) plugin JACoP28.

Statistics

All statistical analysis was performed using IBM SPSS 22.0.0.0, or Graph Pad Prism 5.01. Statistical significance was tested with Student's two-tailed paired or unpaired t-tests, two-tailed Mann Whitney tests, repeated measures ANOVA, or a generalized log-linear mixed model with random effect of animal (autoregressive covariance) and fixed effect of treatment group, week, and the interaction of treatment group and week. All data are shown as mean

±sem, with individual animals also shown. The choice of parametric or non-parametric test followed a Kolmogorov-Smirnov test with the Dallal-Wilkinson-Lilliefor corrected p value. Significance level was set to an α-error of $p<0.05$.

Supplementary Material

Refer to Web version on PubMed Central for supplementary material.

Acknowledgements

We thank G. Schiavo (UCL Institute of Neurology) for the gift of tetanus toxin, and S. Hart (UCL Institute of Child Health) for the mouse Neuro-2a cell line. We are grateful to J. Cornford for assistance with ECoG analysis, and K. Hashemi for help optimizing wireless transmitter use. This project was supported by the European Union's Horizon 2020 research and innovation program under the Marie Skłodowska-Curie Grant Agreement No. 701411 to AL, and by grants from the Medical Research Council to DMK, SS and MCW (MR/L01095X/1), and from the Wellcome Trust to DMK (095580/Z/11/Z) and DMK and SS (104033/Z/14/Z).

References

1. Chen Z, Brodie MJ, Liew D, Kwan P. Treatment Outcomes in Patients With Newly Diagnosed Epilepsy Treated With Established and New Antiepileptic Drugs: A 30-Year Longitudinal Cohort Study. JAMA Neurol. 2018; 75:279–286. [PubMed: 29279892]
2. Kullmann DM, Schorge S, Walker MC, Wykes RC. Gene therapy in epilepsy-is it time for clinical trials? Nature reviews. Neurology. 2014; 10:300–304. [PubMed: 24638133]
3. Kwan P, Schachter SC, Brodie MJ. Drug-resistant epilepsy. The New England journal of medicine. 2011; 365:919–926. [PubMed: 21899452]
4. Tang F, Hartz AMS, Bauer B. Drug-Resistant Epilepsy: Multiple Hypotheses, Few Answers. Front Neurol. 2017; 8:301. [PubMed: 28729850]
5. Perucca P, Gilliam FG. Adverse effects of antiepileptic drugs. The Lancet. Neurology. 2012; 11:792–802. [PubMed: 22832500]
6. Ryvlin P, Cross JH, Rheims S. Epilepsy surgery in children and adults. The Lancet. Neurology. 2014; 13:1114–1126. [PubMed: 25316018]
7. Wykes RC, et al. Optogenetic and potassium channel gene therapy in a rodent model of focal neocortical epilepsy. Science translational medicine. 2012; 4:161ra152.
8. Katzel D, Nicholson E, Schorge S, Walker MC, Kullmann DM. Chemical-genetic attenuation of focal neocortical seizures. Nature communications. 2014; 5:3847.
9. Cook MJ, et al. Prediction of seizure likelihood with a long-term, implanted seizure advisory system in patients with drug-resistant epilepsy: a first-in-man study. The Lancet. Neurology. 2013; 12:563–571. [PubMed: 23642342]
10. Baldassano SN, et al. Crowdsourcing seizure detection: algorithm development and validation on human implanted device recordings. Brain : a journal of neurology. 2017; 140:1680–1691. [PubMed: 28459961]
11. Buckingham SC, et al. Glutamate release by primary brain tumors induces epileptic activity. Nature medicine. 2011; 17:1269–1274.
12. During MJ, Spencer DD. Extracellular hippocampal glutamate and spontaneous seizure in the conscious human brain. Lancet. 1993; 341:1607–1610. [PubMed: 8099987]
13. Stephens ML, et al. Tonic glutamate in CA1 of aging rats correlates with phasic glutamate dysregulation during seizure. Epilepsia. 2014; 55:1817–1825. [PubMed: 25266171]
14. Cavus I, et al. 50 Hz hippocampal stimulation in refractory epilepsy: Higher level of basal glutamate predicts greater release of glutamate. Epilepsia. 2016; 57:288–297. [PubMed: 26749134]
15. Thomas PM, Phillips JP, O'Connor WT. Hippocampal microdialysis during spontaneous intraoperative epileptiform activity. Acta Neurochir (Wien). 2004; 146:143–151. [PubMed: 14963746]

16. Frazier SJ, Cohen BN, Lester HA. An engineered glutamate-gated chloride (GluCl) channel for sensitive, consistent neuronal silencing by ivermectin. The Journal of biological chemistry. 2013; 288:21029–21042. [PubMed: 23720773]
17. Yaguchi M, et al. Characterization of the properties of seven promoters in the motor cortex of rats and monkeys after lentiviral vector-mediated gene transfer. Hum Gene Ther Methods. 2013; 24:333–344. [PubMed: 23964981]
18. Barker-Haliski M, White HS. Glutamatergic Mechanisms Associated with Seizures and Epilepsy. Cold Spring Harb Perspect Med. 2015; 5:a022863. [PubMed: 26101204]
19. Tzingounis AV, Wadiche JI. Glutamate transporters: confining runaway excitation by shaping synaptic transmission. Nature reviews. Neuroscience. 2007; 8:935–947. [PubMed: 17987031]
20. Vink CA, et al. Eliminating HIV-1 Packaging Sequences from Lentiviral Vector Proviruses Enhances Safety and Expedites Gene Transfer for Gene Therapy. Molecular therapy : the journal of the American Society of Gene Therapy. 2017; 25:1790–1804. [PubMed: 28550974]
21. Mainardi M, Pietrasanta M, Vannini E, Rossetto O, Caleo M. Tetanus neurotoxin-induced epilepsy in mouse visual cortex. Epilepsia. 2012; 53:e132–136. [PubMed: 22577757]
22. Cleeren E, Casteels C, Goffin K, Janssen P, Van Paesschen W. Ictal perfusion changes associated with seizure progression in the amygdala kindling model in the rhesus monkey. Epilepsia. 2015; 56:1366–1375. [PubMed: 26174547]
23. Weir GA, et al. Using an engineered glutamate-gated chloride channel to silence sensory neurons and treat neuropathic pain at the source. Brain : a journal of neurology. 2017; 140:2570–2585. [PubMed: 28969375]
24. Jaenisch N, et al. Reduced tonic inhibition after stroke promotes motor performance and epileptic seizures. Scientific reports. 2016; 6:26173. [PubMed: 27188341]
25. Asztely F, Erdemli G, Kullmann DM. Extrasynaptic glutamate spillover in the hippocampus: dependence on temperature and the role of active glutamate uptake. Neuron. 1997; 18:281–293. [PubMed: 9052798]
26. Cavus I, et al. Extracellular metabolites in the cortex and hippocampus of epileptic patients. Annals of neurology. 2005; 57:226–235. [PubMed: 15668975]
27. Miles R, Blaesse P, Huberfeld G, Wittner L, Kaila K. Chloride homeostasis and GABA signaling in temporal lobe epilepsyJasper's Basic Mechanisms of the Epilepsies. Bethesda (MD): 2012. (eds. th, et al.)
28. Bolte S, Cordelieres FP. A guided tour into subcellular colocalization analysis in light microscopy. J Microsc. 2006; 224:213–232. [PubMed: 17210054]

Europe PMC Funders Author Manuscripts

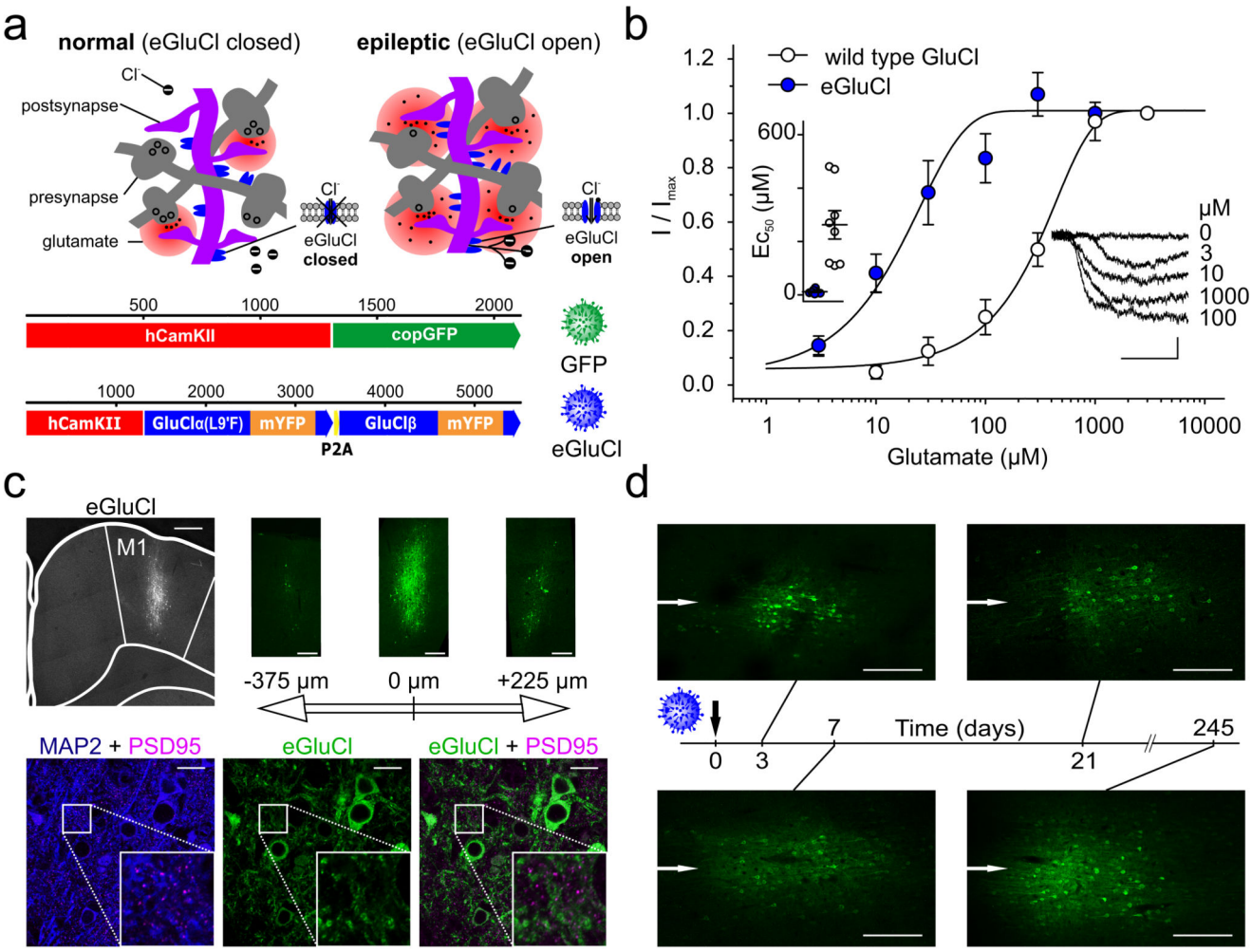

Figure 1. Mode of action and glutamate sensitivity of eGluCl.

(a) Top: proposed mode of action of eGluCl. eGluCl biochemically senses increased glutamate concentrations during impending seizures, and subsequently silences neurons by opening an inhibitory Cl^- conductance. Bottom: lentiviral transfer plasmid design. **(b)** Electrophysiological characterization of glutamate sensitivity of wild type GluCl and eGluCl in Neuro-2a cells. Left inset: estimated EC_{50} in individual experiments (wild type: 262±53μM, n=8 cells; eGluCl: 12±3μM n=8 cells; mean±sem, $p<0.001$, Student's t-test). Right inset: glutamate-evoked currents from a representative experiment (scale bar 0.5sec and 0.1nA). **(c)** Immunolabeling of eGluCl after injection in primary motor cortex (M1) indicates a spread of around 700 μm (left image, M1 region is indicated, scale bar 500μm). The three images on the right show slices from the same brain at position -375, 0, and +225μm anterior and posterior to the eGluCl injection site respectively (scale bar 250μm). The bottom three images show MAP2 + PSD95 (left) to map the cell shape and synapse location, eGluCl (middle), and eGluCl + PSD95 to map eGluCl expression at the synapse (right) (scale bar 20μm). Approximately 0.29±0.01% of eGluCl occurred at PSD95 puncta, and conversely 13.50±2.49% of PSD95 co-localized with eGluCl in transduced areas of the brain (Pearson's correlation coefficient: 0.19±0.03, n=3 animals). **(d)** Expression pattern of

eGluCl at different time points (3, 7, 21, and 245 days) post–Rx (scale bar 250μm) (representative images from n=2 animals). The white arrows indicate the injection needle track.

note

Europe PMC Funders Author Manuscripts

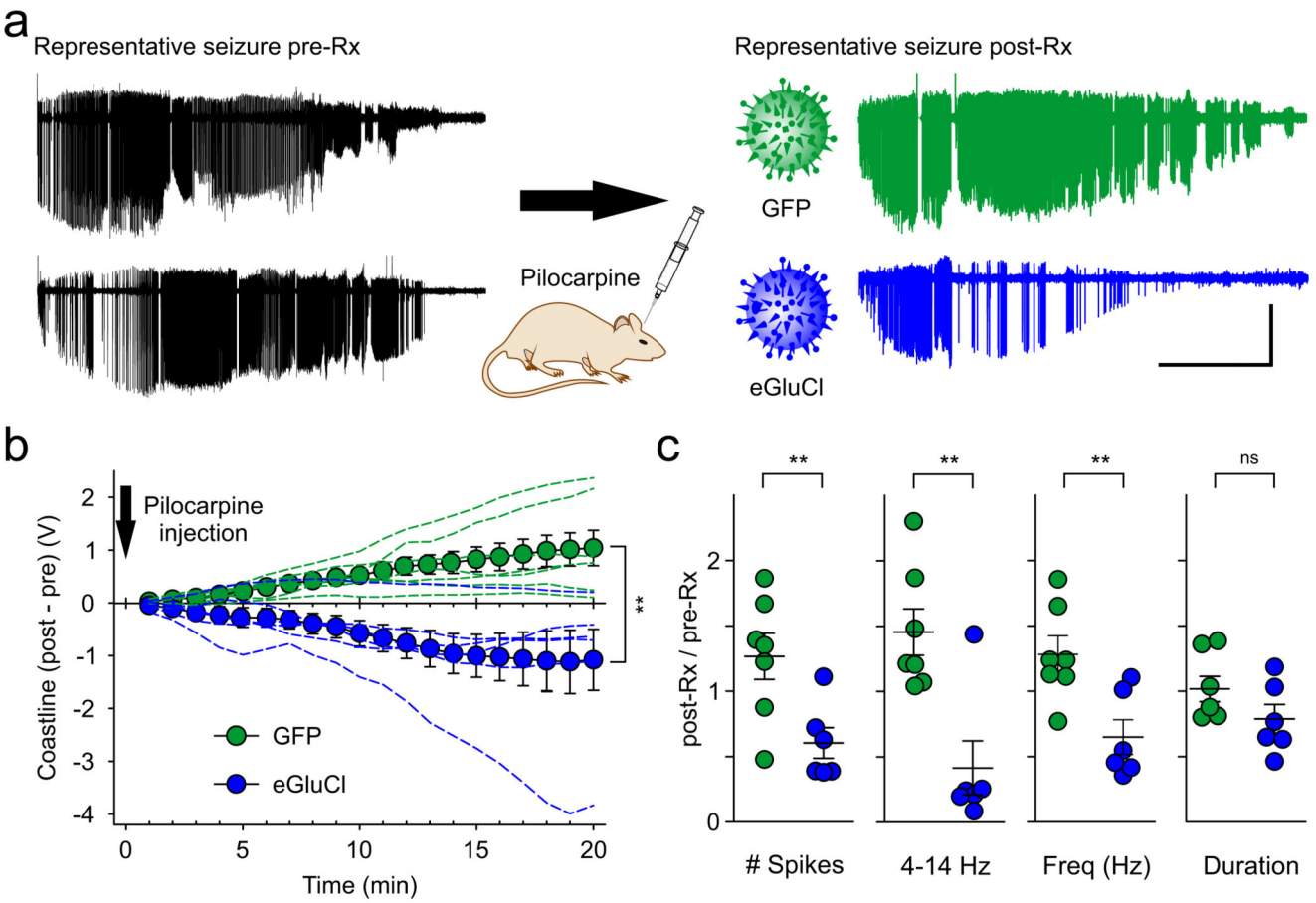

Figure 2. eGluCl reduces acute chemoconvulsant-induced seizures.

(a) Representative seizures elicited by focal pilocarpine injection before (pre-Rx) and after lentiviral treatment with eGluCl or GFP (post-Rx) (scale bar 5min and 1mV). **(b)** Absolute differences in the cumulative coastline between the two pilocarpine trials pre-Rx and post-Rx (eGluCl –1.08±0.58V at 20 minutes, n=6 animals; GFP 1.04±0.34V, n=7 animals; mean ±sem, p=0.007, Student's t-test). **(c)** Number of spikes (ratio of spikes in the second trial to the first trial: eGluCl: 0.60±0.12; GFP: 1.27±0.18; mean±sem, p=0.012, Student's t-test), 4 – 14 Hz power (ratio of second trial to first: eGluCl: 0.44±0.19; GFP: 1.47±0.16; p=0.002), spike frequency (ratio of second trial to first: eGluCl: 0.65±0.13; GFP: 1.29±0.14; p=0.007), and seizure duration post-Rx normalized to the corresponding values pre-Rx (ratio of second trial to first: eGluCl: 0.79±0.11; GFP: 1.02±0.10; p=0.146). *p<0.05; **p<0.01.

Europe PMC Funders Author Manuscripts

Europe PMC Funders Author Manuscripts

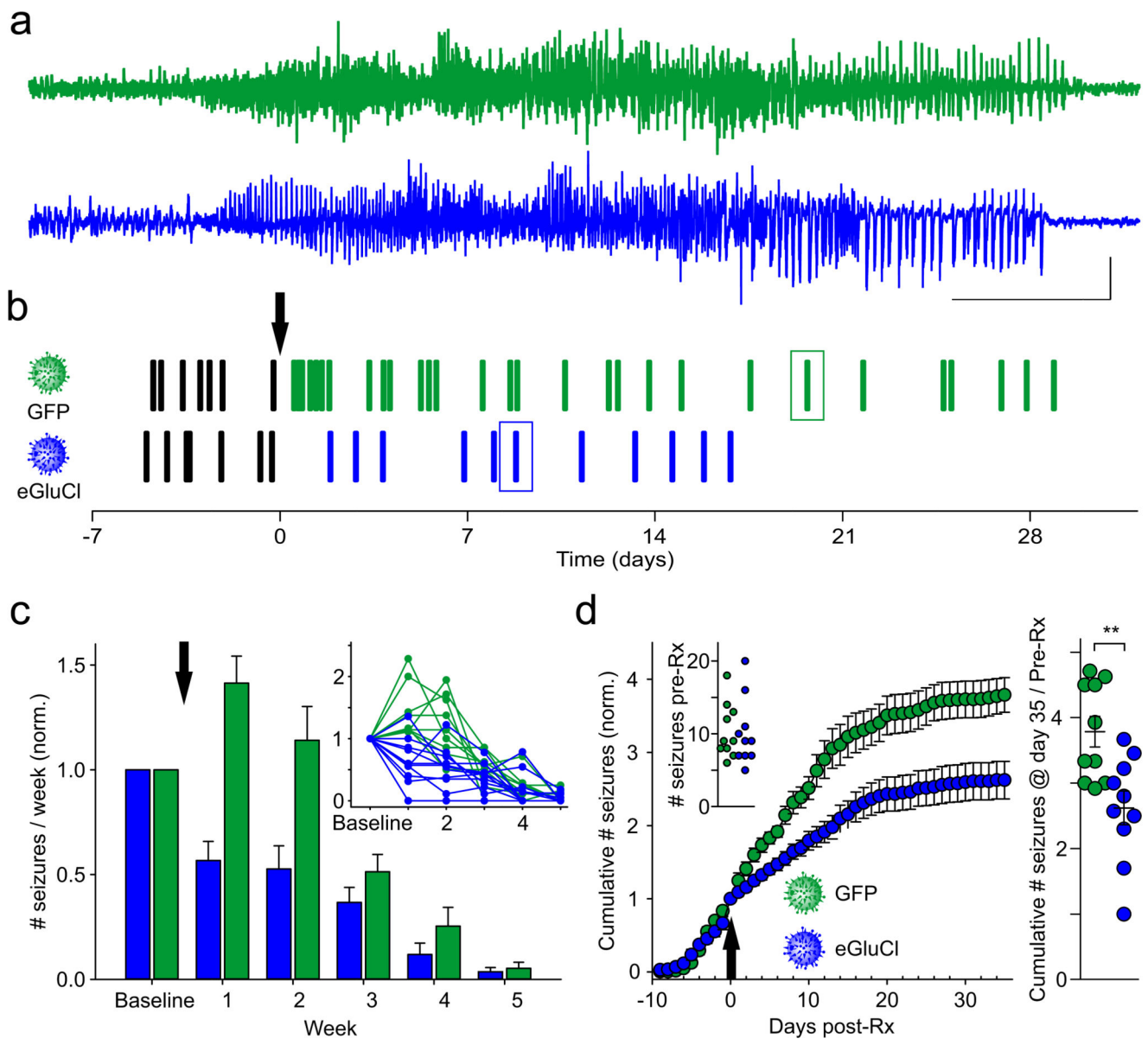

Figure 3. eGluCl reduces the absolute number of seizures in a model of chronic focal neocortical epilepsy.

(a) Representative seizures from two animals injected with tetanus toxin into layer 5 of the visual cortex after treatment with eGluCl or control GFP lentivector. (scale bar 10sec and 0.5mV). **(b)** Raster plot of seizures in the same animals. Boxes: seizures in panel (a). TetTx was injected at surgery (day -11), and the arrow indicates the timepoint of either eGluCl or GFP lentivector injection (day 0). **(c)** Seizure frequency (per week, mean±sem) for animals treated with either eGluCl (n=10 animals) or control GFP lentivector (n=10 animals) (indicated by the arrow), normalized by pre-Rx seizure rates (generalized log-linear mixed model: $F(1, 59)=20.66$, treatment effect $p<0.001$; $F(8, 59)=17.28$, treatment*week interaction effect $p<0.001$). The inset shows all individual experiments. **(d)** Normalized cumulative seizure frequency (per day) for animals injected with either eGluCl or control

GFP lentivector (mean±sem). Inset: absolute number of seizures pre-Rx for the two groups (eGluCl 10.1±1.5, n=10; GFP 10.4±1.2, n=10; mean±sem, p=0.761, Student's t-test). The arrow indicates the timepoint of eGluCl or GFP injection. Right panel: total number of seizures post-Rx, normalized by pre-Rx rate, for animals injected with either eGluCl or GFP control (eGluCl: 2.62±0.26, n=10; GFP: 3.79±0.24, n=10; mean±sem, p=0.004, Student's t-test). **p<0.01.

Europe PMC Funders Author Manuscripts

Europe PMC Funders Author Manuscripts

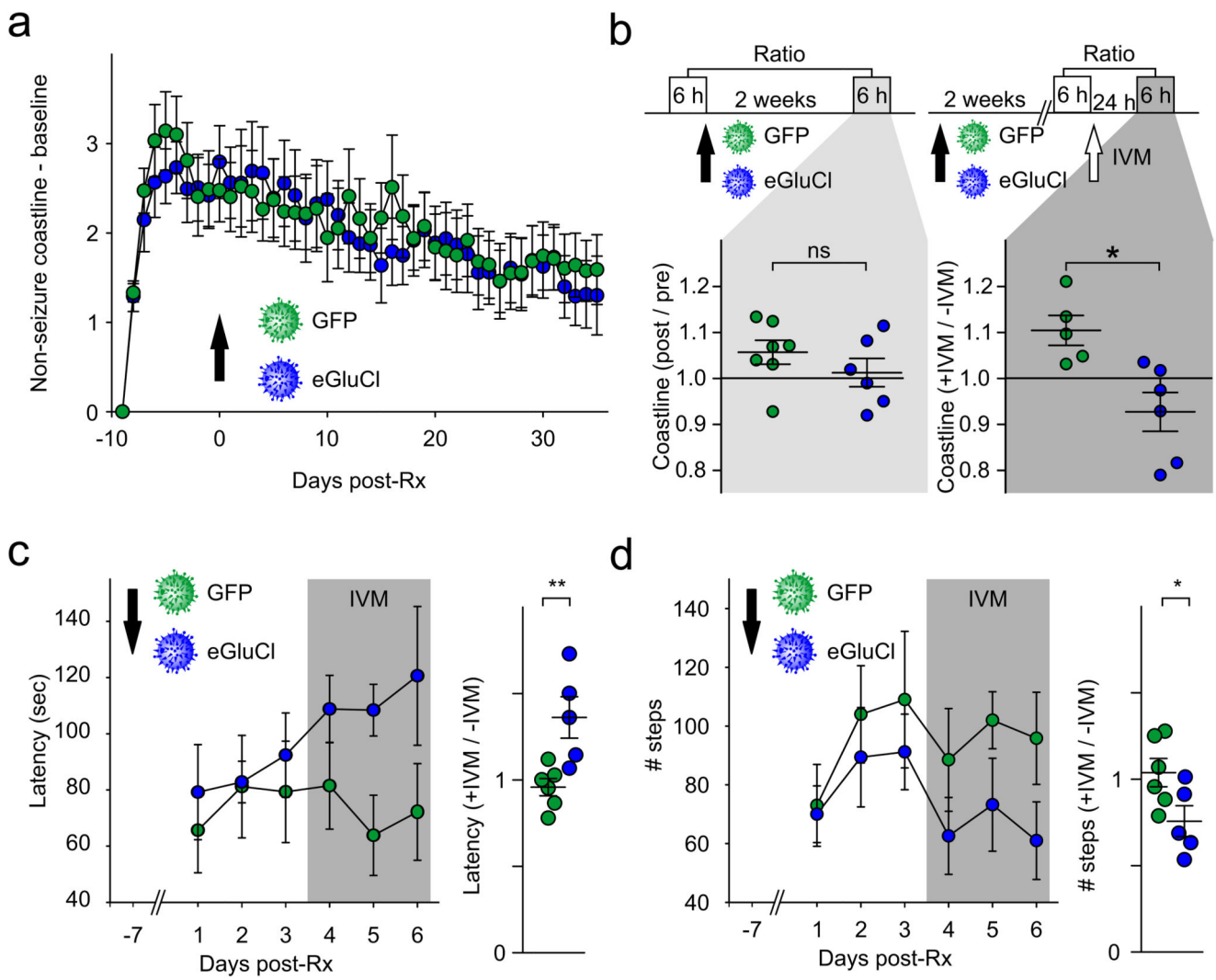

Figure 4. eGluCl treatment has no effect on normal brain function.

(a) Absolute increase in ECoG coastline after TetTx injection (day -10), excluding seizures, showing no difference between eGluCl and GFP treatment at day 0 (mean±sem, same animal cohort as in Figure 3). **(b)** Effect of GFP or eGluCl treatment on ECoG coastline evaluated over two 6 h periods (no TetTx). Top: experimental design. The lower panels show the coastline after GFP or eGluCl treatment normalized by pre-Rx coastline (left) (ratio: eGluCl: 1.01±0.03, n=7; GFP: 1.06±0.03, n=6; mean±sem, p=0.293, Student's t-test), or the post-Rx coastline after 5mg/kg ivermectin injection (+IVM), normalized by the baseline before ivermectin (-IVM) (ratio: eGluCl: 0.93±0.04, n=6; GFP: 1.10± 0.03, n=5; mean±sem, p=0.010, Student's t-test). *p<0.05. **(c)** Post-Rx latency to fall from the accelerating rotarod on three consecutive days (average latency to fall in 3 rotarod sessions eGluCl: 84.8±12.0sec, n= 5; GFP: 75.4±15.0 sec, n=6; mean±sem, p=0.646, Student's t-test), and subsequently on three days 24h after IVM (gray). The right panel shows the average latencies after IVM normalized to the average of the 3 test sessions before IVM (eGluCl: 1.36±0.12, n = 5, GFP: 0.96±0.05, n=6; mean±sem, p=0.009, Student's t-test). **p<0.01. **(d)**

Post-Rx absolute number of steps taken on an elevated grid (eGluCl: 83.5±12.7; GFP: 95.3±17.5; mean±sem, p=0.612, Student's t-test), and subsequently after IVM (same animals as in (c)). The right panel shows the number of steps after IVM normalized to the average of the 3 test sessions before IVM (expressed as a ratio of steps taken pre-IVM, eGluCl: 0.76±0.09, n = 5; GFP: 1.04±0.08, n=6; mean±sem, p=0.045, Student's t-test). *p<0.05.

Europe PMC Funders Author Manuscripts